[5]

The first neutron time-of-flight line in Spain: commissioning and new data for the definition of a neutron standard field

M. Macías, B. Fernández

Centro Nacional de Aceleradores (Universidad de Sevilla, Junta de Andalucía, CSIC)
E-41092, Sevilla, Spain
Departamento de Física Atómica, Molecular y Nuclear
Universidad de Sevilla
E-41012, Sevilla, Spain

J. Praena

Departamento de Física Atómica, Molecular y Nuclear
Universidad de Granada,
E-18071, Granada, Spain

Abstract

The National Accelerator Laboratory (CNA) has installed the first accelerator line in Spain devoted to the measurement of cross sections involving neutrons by means of the time-of-flight technique. For the neutron generation, pulsed proton beams with 1 nsec pulse width and with variable repetition rates are delivered. The acquisition system is based on CAEN Digitizer. The aim of this work is to demonstrate the good performance of the whole time-of-flight system at CNA. The commissioning of the line has consisted of the measurement of the well-known neutron field generated by protons at 1912 keV impinging on a thick lithium target. Such field has been extensively used in nuclear astrophysics since 1988. Recently, there have been experimental works with the goal to support it as a standard neutron field. The results of the present work shows the good performance of the time-of-flight system and also support the possible definition of such neutron field as standard.

Keywords: Time-of-flight technique, accelerator-based neutron source, standard neutron field

1. Introduction

Accelerator-based neutron sources (ABNS) play an important and complementary role to large neutron facilities. ABNS can be applied to material science, neutron instrumentation and analysis, education, nuclear astrophysics or single event effect (SEE) studies on electronics devices (Colonna et al., 2018). In Spain the most important nuclear physics laboratory is the National Accelerator Laboratory (CNA) sited in Seville (García et al., 2000). CNA houses a 3 MV Tandem Pelletron model 9SDH-2 with seven experimental lines (NEC, 2019). In 2013, the multipurpose nuclear line started to be used for neutron generation by means of two reactions ^{7}Li(p,n)^{7}Be and ^{2}H(d,n)^{3}He. Thenceforth, HiSPANoS (HiSPAlis Neutron Source), the first ABNS in Spain began to operate. Since then several experiments have been carried out in continuous beam. Fast neutrons were used for the study of SEE in SRAM memories with the conclusion that 8T cells have a better performance against irradiation than 6T cells (Malagón et al., 2017). Thermal neutrons were used for the characterization of dosimeters to be utilized in conventional radiotherapy halls (Praena et al., 2015; Irazola et al., 2016). Stellar neutron spectra were produced for determining the Maxwellian-averaged cross section (MACS) of ^{181}Ta(n,γ) (Praena et al., 2013). Also the MACS of ^{159}Tb(n,γ) was measured and the implications in the s-process abundance distributions in the radiative C13-pocket layers of a 3$M_\odot$ star were studied (Praena et al., 2014).

With regard to nuclear astrophysics, experimental studies on the MACS of ^{197}Au(n,γ) at kT= 30 keV were carried out at CNA with the aim to solve a long term discrepancy between the evaluation of standards and the historical value provided by Ratynski and Käppeler (R&K) (Ratynski et al., 1988). The MACS of ^{197}Au(n,γ) at kT= 30 keV of R&K has been extensively used as reference in experiments devoted to nuclear astrophysics. Recently, the results of the studies at CNA (Jiménez-Bonilla et al., 2014) have been confirmed by the evaluation of the IAEA (Carlson et al., 2018). In fact, at present, all the nuclear data for astrophysics obtained using the MACS of ^{197}Au(n,γ) at kT= 30 keV of R&K as reference are being renormalized to the new value provided by KaDoNiS data base (Dillmann et al., 2014).

In relation to the present work, the MACS of ^{197}Au(n,γ) at kT= 30 keV was obtained by R&K with a neutron field produced by protons at 1912 keV impinging on a thick lithium target. Such neutron field has been very important in nuclear astrophysics because it resembles in good approximation the stellar field in important nucleosynthesis scenarios (Ratynski et al., 1988). Hence, it has been used for measuring several MACS (Dillmann et al., 2014). In the last years, there has been some experimental works for establishing the R&K field as a neutron standard (Lederer et al., 2012). The consistent experimental results of the neutron field obtained by R&K (Ratynski et al., 1988), Lederer et al. (Lederer et al., 2012) and Feinberg et al. (Feinberg et al., 2012) have shown the robustness of the method. The three experiments needed a good time resolution for an accurate determination of the neutron field which ranges from 0 to 110 keV. In particular, a high energy resolution is needed for an accurate determination of the neutron spectra at different angles. The only experimental technique with such energy resolution for neutrons is the time-of-flight (TOF) technique which was used in the mentioned experiments. Therefore, the measurement of the well-known, not yet standard, neutron field of R&K is an excellent test of the TOF system developed at CNA for neutrons.

The TOF technique with neutrons needs a pulsed and bunched beam in time with a pulse width low enough or with a flight path large enough (or both) for achieving the necessary energy resolution. It is straightforward that the facility characteristics and the experimental setup determine the achievable energy resolution. Thus, the selected parameters in a TOF experiment depend on several ones as the flight path, flux, beam time within practical limits or detector efficiency. In case of spallation facilities, as n_TOF at CERN, large flight paths are possible (Gunsing et al., 2016). However, for accelerators as the Tandem at CNA, the high energy resolution must be achieved with the shortest possible pulse width of the proton beam. Briefly, in experiments and facilities similar to the CNA, a good energy resolution can be achieved with pulse widths from 1 to 3 ns (FWHM) and flight paths from 50 to 100 cm which keep a reasonable neutron flux. The repetition rate must be optimized to maximize the count rate avoiding the overlap between the slowest neutrons of a pulse and the fastest neutrons of the successive pulse. For all these purposes a pulsing and bunching system was installed at the low energy of the accelerator at CNA and a new line was designed and installed. The system consists of a chopper and a buncher. The chopper deflects the protons producing a 60 ns beam with the capability to work at repetition rates from 62.5 kHz to 2 MHz. Then, the 60 ns beam enters in the buncher which compresses it to 1 ns by means of a radiofrequency at 8 MHz. Regarding the TOF line, it holds the conventional elements for the transmission and the focalization of the ion beam. The most relevant is a capacitive pickup which is the last element just before the neutron production target. It was designed as a ring shaped phase probe of 50 Ω impedance. The output signal of the pickup gives information of the integral charge per pulse, the frequency of the pulses, the time width and the noise-to-signal ratio. The whole system was successfully tested and proton beams with 1 ns pulse width were measured for variable repetition rates (Macías et al., 2018).

The goal of the present work is to validate the complete TOF system for neutrons at CNA. For this, the so-called R&K neutron field produced by the ^{7}Li(p,n)^{7}Be reaction at E_p=1.912 MeV with thick target is measured and compared with previous works. In addition, the results obtained at CNA could contribute to the future definition of the R&K neutron field as a standard. The applications of such field include astrophysics and validation of evaluated data for the Generation IV of nuclear reactors, dosimetry and radioprotection (Praena et al., 2014).

2. Experiment

2.1. The ^{7}Li(p,n)^{7}Be reaction and the setup

The ^{7}Li(p,n)^{7}Be reaction has been widely used in accelerator-based neutron sources because it provides a comparably large flux of neutrons in the range between a few keV and several hundreds keV. There are a variety of experiments providing data of the neutron emission in energy and in angle of the ^{7}Li(p,n)^{7}Be reaction. Specially, it has been studied the energy range above the reaction threshold (1.881 MeV) where the cross section reaches a value of 270 mb and a broad resonance at 2.25 MeV increases the cross section up to 580 mb (Macklin et al., 1958). In particular, Liskien and Paulsen reviewed and tabulated the laboratory differential cross sections as functions of the proton energy and neutron emission angle (Liskien et al., 1975). Later, Lee and Zhou developed a method for computing angular distributions, energy spectra and total yields for proton energies up to 2-2.5 MeV for thick and thin targets of metallic lithium and lithium compounds (Lee et al., 1999).

In particular, when a monochromatic proton beam impinges on a thick lithium target, the protons are slowed down to the threshold producing a continuous neutron spectrum. It has been widely reported that 8 μm of lithium are enough to slow down to the threshold at 1912 keV proton energy (Ratynski et al., 1988). At 1912 keV, the kinematics of the ^{7}Li(p,n)^{7}Be reaction and the experimental data (Liskien et al., 1975) (Lee et al., 1999) show that the neutrons are forward emitted in a cone of $\approx 60°$ of aperture, see Figure 1. Thus, the spectrum at the production point can be determined by measuring the neutron spectra at different forward angles and, then, scaling each spectrum by the respective solid angle (Ratynski et al., 1988).

With a similar setup to R&K, our experiment was performed at the TOF line of the 3 MV Tandem at CNA. The proton current delivered by the accelerator in continuous mode was 10 μA. The accelerator terminal was calibrated by using the 991.86 keV ^{27}Al(p,γ) and 2409 keV ^{24}Mg(p,p'γ) resonances. The calibration was checked several times during the experiment with the threshold of the ^{7}Li(p,n)^{7}Be reaction. For checking the performance of TOF system in different configurations, the chopper operated at 62.5 kHz for two flight paths, 50 and 35 cm, and at 500 kHz for 50 cm flight path.

The experimental setup consisted of a goniometer made of aluminum holders for a precise location of the detectors in angle and a target assembly accomplished to the beam pipe of the TOF line. Figure 1 shows a scheme of the experimental setup. The target assembly consisted of an aluminum cylinder (4.2-cm diameter and 15-cm long) and a copper backing for the lithium target. The metallic lithium needs a careful handling due to its chemical instability and strong oxidation potential. The lithium target was prepared by forced pressure onto the copper backing and it was always stored in inert gas. The lithium thickness was around 120 μm, therefore, protons were completely stopped inside the lithium. The lithium diameter was 1 cm and the proton beam was focused and collimated to a diameter less than 0.5 cm. The copper backing had a circular shape with a diameter of 4 cm and a thickness of 0.5 mm and it was directly connected to the target assembly with an O-ring. The target assembly was connected to the beam pipe of the TOF line. The only materials that neutron beam found from the source to the detectors were the copper backing and the lithium. The copper backing holding the lithium target was cooled by a forced air flow on the external side. The pressure was $\approx 10^{-6}$ mbar during the whole experiment. This setup was carefully designed in an attempt to minimize the neutron scattering. The lithium target was located at the center of goniometer with movable stands for placing ^{6}Li-glass detectors purchased from Scionix Ltd. (Scionix). The detectors were located at the same height of the lithium target. A movable ^{6}Li-glass detector (5.08-cm diameter and 2.54-cm thick) recorded the signals at 0°, 15°, 30°, and 45° and 60° at a flight path of 50 cm. A second movable detector (5.08-cm diameter and 1.27-cm thick) recorded the signals at 0° and at 60° at a shorter flight path of 35 cm. A third ^{6}Li-glass detector was used as monitor at a fixed position with no geometrical interference with the others. Figure 1 shows a scheme of the experimental setup.

2.2. Data acquisition

The signals from the photomultiplier of each detector were processed with the DT5730 Desktop of CAEN, a 8 channels 14 bit at 500 Ms/s FLASH ADC Waveform Digitizer (CAEN, 2016). The signals induced by the proton beam in the pickup were used as the start signal for the acquisition. Then, a time

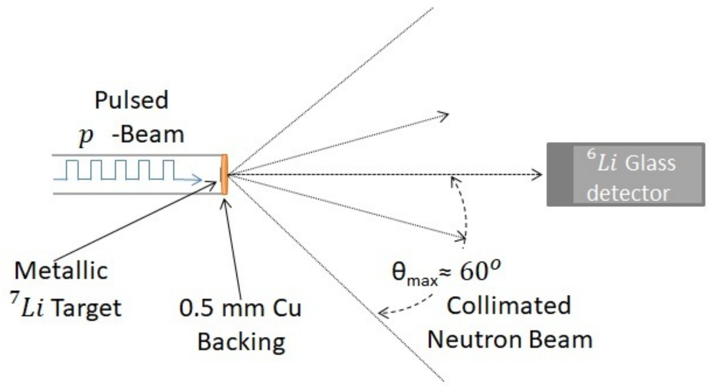

Figure 1: Scheme of the experimental setup and technique.

acquisition window of 1500 ns with 2 ns per channel was opened collecting the mentioned signals from the detectors. The acquisition was triggered independently by the signals of each detector. The trigger enables the event building, that includes the waveforms (i.e. the raw samples) of the input, the trigger time stamp, the baseline, and the integral charge (IC) of the signals within the time window which covered their whole duration (CAEN, 2016). The DT5730 allows on-line visualization of the one-dimensional (1D) TOF histogram and the one-dimensional IC histogram.

During the acquisition, the data are continuously written in a circular memory buffer. When the trigger occurs, the digitizer writes further samples for the post trigger and freezes the buffer that can be read by one of the provided readout links. This acquisition can acquired continuously without any dead time in a new buffer (CAEN, 2016). Digitized signals are transmitted via an USB connection and stored in a computer for off-line analysis. Figure 2 shows a 1D histogram of the IC of a ^{6}Li-glass detector during the present experiment. An excellent discrimination between γ-rays and neutrons was achieved. Therefore, the background level associated to γ-rays and electronic noise can be reduced by setting a threshold in the IC without any lost of neutrons.

The TOF technique for neutrons is based on the discrimination of their energies due to their different flight times from the production target to the

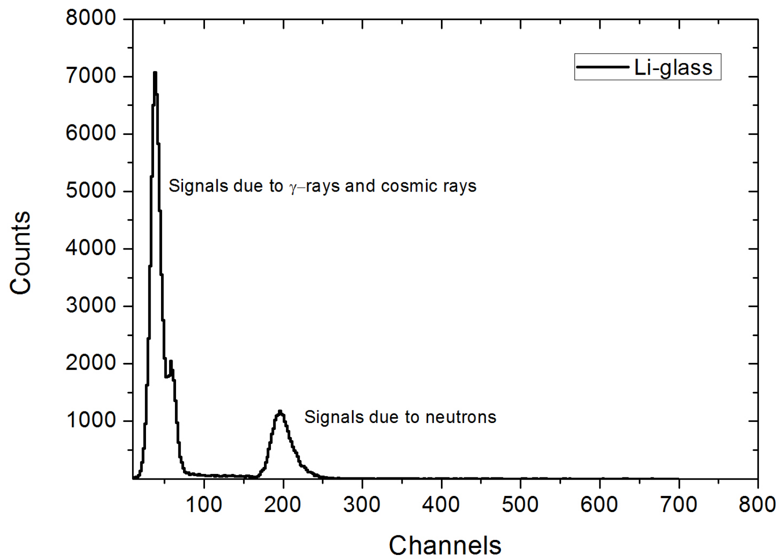

Figure 2: Raw data organized in 1D histogram of the integral charge (IC) in the ^{6}Li-glass detector.

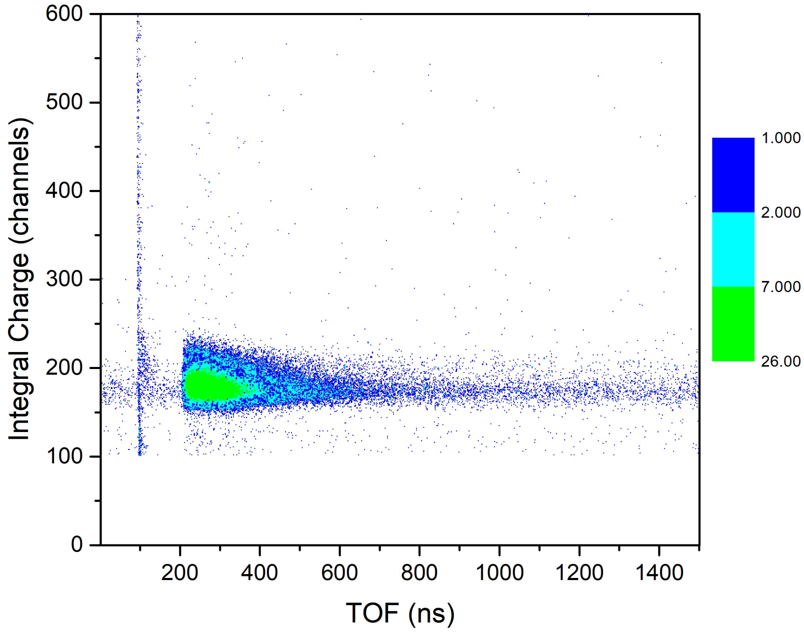

Figure 3: Raw data organized in a 2D spectrum TOF vs IC. The color scheme indicates the number of counts per pixel.

point where the reaction takes place. ^{6}Li-glass detectors are sensitive to γ-rays and neutrons as shown in Figure 2. It is straightforward that the created γ-rays in the ^{7}Li(p,n)^{7}Be reaction propagate at the speed of light and the velocity of the neutrons depends on their energy. Figure 3 shows a two-dimensional scatter plot of the TOF versus the IC of the signals. The γ-rays appear as a vertical line in time at 150 ns. The neutrons appear in the horizontal band from approximately 200 to 700 ns with a drop shape. It can be noticed the excellent discrimination between γ-rays and neutrons during the experiment. Also, it can be noticed that signals are scattered over all the TOF vs IC regions. This background was carefully studied, analyzed and subtracted as it is discussed in the next section.

3. Data analysis

The intrinsic efficiency of a ^{6}Li-glass detector is mainly defined by the ^{6}Li(n,t)^{4}He reaction. However, the presence of neutron resonances in the measured energy range in some of the materials of the detector must be carefully studied. The experiment of Lederer et al (Lederer et al., 2012) carried out with analogous detectors showed a small contribution to the intrinsic efficiency of resonances of ^{56}Fe and ^{28}Si which are also present in the Borosilicate, μ-metal and tape of our detectors. Our detectors were purchased to Scionix Ltd. (Scionix) with a sheet which detailed the geometry and the materials. The effect of the materials was studied by means of Monte Carlo simulations using a detailed model of the detectors with MCNPX (MCNPX code, 2005). Figure 4 shows the simulated intrinsic efficiency. Smalls dips due to the mentioned resonances can be noticed. For the conversion from TOF to neutron energy the complete setup must be carefully simulated. This conversion is associated to a particular experiment and the induced processes by the neutrons in the target assembly, goniometer and detectors before they produce the ^{6}Li(n,t)^{4}He reaction. All these processes were simulated with MCNPX.

As shown in Figure 3, the presence of scattered signals over the TOF vs IC regions involve a background that must be subtracted. The origin of the background was mainly due to the scattered neutrons in the experimental hall. The neutron target was positioned at 6 meters of the wall located in the direction of the beam, and at 5 and 20 meters from the walls on the right and on left in parallel to the direction of the beam, respectively. The ceiling was at 10 meters from the target and the floor was at 1.25 meters from the target. The walls, the floor and the ceiling are made of concrete. In order to extract the background, its dependence as a function of the energy or its possible correlation with the time had to be determined. With this aim, the detectors were shielded with shadow bars and the TOF spectra were recorded at each angular position. The shadow bar was made of polyethylene with a cylindrical shape of 5.08 cm diameter and 20 cm length. Figure 5 shows a comparison between a TOF histogram

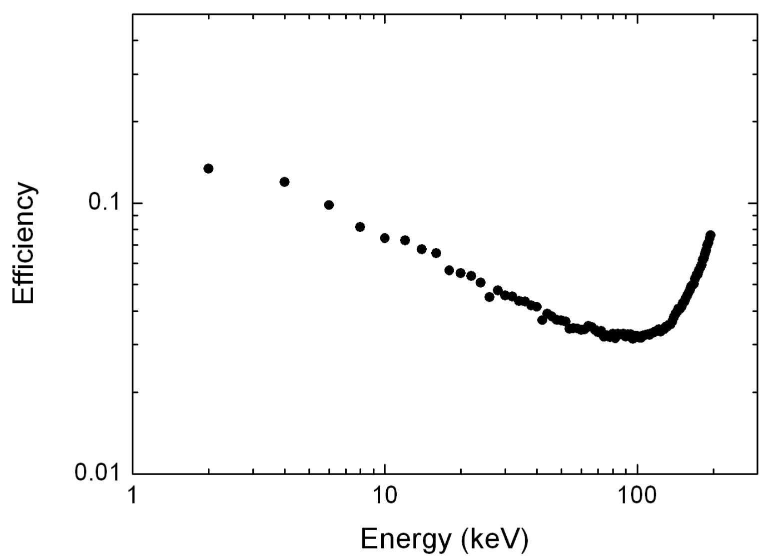

Figure 4: Intrinsic efficiency of a ^{6}Li-glass detector (5.08-cm diameter and 2.54-cm thick) for neutron detection determined with the MCNPX simulation code.

with shadow bar (black line) and without shadow bar (red line). For both spectra, the peak close to ≈150 ns corresponds to the γ-rays produced in the ^{7}Li(p,n)^{7}Be reaction (the so-called γ-flash). The rest of the signals with shadow bar (black line) were due to scattered neutrons and γ-rays in the experimental hall. The conclusion is that the background was found to be very small and uncorrelated with the time. This conclusion was supported by TOF histograms acquired at 70° for which only scattered neutrons were detected as expected due to the kinematics of the reaction. Regarding the TOF histogram without shadow bar (red line), the onset of neutrons events is located around to 200 ns. An excellent separation in time between neutrons and γ-flash is shown. Similar TOF histograms were acquired for all the angles. It should be noticed that the flat background in time is also defined in the region between the γ-flash and the onset of the neutron events (red line). Thus, for each angle a flat background was subtracted to the corresponding TOF histogram. Then, the TOF histograms were converted to energy as mentioned before.

In this experiment the uncertainty was mainly dominated by the statistical one. Thereby in the analysis, energy bins of 5 keV were chosen as a good compromise between enough energy resolution and a minimization of the statistical uncertainty. Briefly, at 0° position the statistical uncertainty ranged from ≈3 to ≈8% and at the larger angles, 45°-60°, ranged from ≈12 to ≈20%. The uncertainty related to the TOF-energy conversion was estimated by the comparison of two energy distributions for each angle and detector. The first one consisted of the simulation of the TOF spectra acquired by the detector and the subsequent application of the TOF-energy conversion. For this, the analytical descriptions of the reaction kinematics of the ^{7}Li(p,n)^{7}Be reaction at E_p=1912 keV of Lee and Zhou (Lee et al., 1999) were introduced in MCNPX for a complete simulation of the experiment. Such analytical descriptions of the differential yield in angle and energy are based on the experimental data of Liskien and Paulsen (Liskien et al., 1975) and they have been programmed by different authors (Mastinu et al., 2009; Reifarth et al., 2009; Friedman et al., 2013). Such procedures have been extensively checked with experimental data

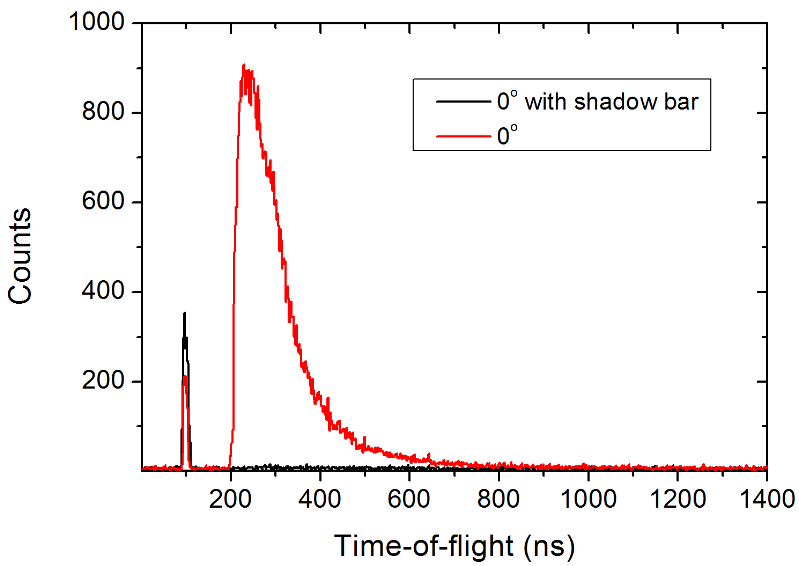

Figure 5: TOF histograms acquired with a ^{6}Li-glass detector at 0° position. Black line corresponds to the detector covered with a shadow bar for avoiding the direct hit of the neutrons on the detector. Red line corresponds to the TOF histogram without shadow bar.

of the ^{7}Li(p,n)^{7}Be reaction (Praena et al., 2014; Lederer et al., 2012; Feinberg et al., 2012). Specifically, we used the procedure already proven in (Praena et al., 2014), in which, a histogram records the simulation of the invested time by the neutrons between the source and the production point of a tritium nucleus inside the detector. The second energy distribution consisted of the energy distribution directly recorded by the detector using the same analytical descriptions of Lee and Zhou (Lee et al., 1999). The comparison between the mentioned energy distributions showed a negligible impact on the total uncertainty, however, a conservative 1% was assumed. Regarding, the uncertainty in the normalization, as mentioned before, a detector was located in a fixed position for a common normalization. The statistical uncertainty associated to the neutron fluence in the monitoring detector was 1.6%.

4. Results and Discussion

In the following, our results will be shown and directly compared with previous measurements of the R&K field. The first comparison regards to the neutron spectra obtained at each angle with particular attention to the 0° spectrum, Figures 6 and 7. The second comparison concerns the angle-integrated spectrum at the neutron production point, Figure 8. For the first one, we compare to Lederer et al. (Lederer et al., 2012) because the data are available on-line and agree with the results of R&K, see EXFOR data base (http://www-nds.iaea.org/exfor/exfor.htm), so, to use Lederer et al. or to use R&K is equivalent. For the second comparison, it is possible to compare directly with R&K (available in EXFOR data base). It is important to point out that both comparisons consist of two facts: the shape of the spectra with particular attention to the maximum energy and the relative intensity of the spectra at the different angles. The intensity of the neutrons depends on the experimental setup, thus, on the proton current, the flight path, etc. For this reason, it is necessary to normalize our results to the results of the Lederer et al. and R&K experiments. In order to ensure the consistency between the angles, we normalized only the area of our spectrum at 0° to the spectrum at 0° of Lederer et al. The rest of our spectra at the different angles were obtained directly from their relative intensity to our normalized 0° spectrum, and then, they are compared with the spectra of Lederer et al. without further normalization.

Figure 6 shows our results of the energy spectra at 0° in bins of 5 keV obtained at different flight paths and repetitions rates in comparison with Lederer et al. (green line). The black line corresponds to 50 cm flight path and 62.5 kHz repetition rate. The red line corresponds to 35 cm flight path and 62.5 kHz repetition rate. The blue line corresponds to 50 cm and 500 kHz repetition rate. Our energy spectra are obtained, as it has been explained, with the background subtraction in the TOF histogram, then, converting them to energy, and finally, applying the corresponding solid angle correction (see below). The good agreement between our results with different flight paths and repetition rates and with the results of Lederer et al. demonstrates the good performance of the whole TOF system for neutrons developed at CNA.

For a proper comparison of the neutron spectra from 0° to 60°, each spectrum has to be scaled by the corresponding solid angle. Indeed, this correction depends on the flight path and the angle between the detector and the target. The scaling factor for each position was calculated by means of accurate MCNPX simulations. Each scaling factor is proportional to the revolution area of the detector around the axis from the center of the target to the center of the detector at 0°. Thus, the correction associated to the 0° spectrum is the most important, or equivalently, the scaling factor is the smallest one. The correction involves relevant decrease of the relative intensity at 0° with regard to the rest of the angles. For this reason, we have discussed it separately from the rest of the angles. In addition, the 0° neutron spectrum is very important because it contains the most energetic neutrons. In fact, in all the activation measurements performed with the method of R&K (Ratynski et al., 1988) the spectrum at 0° was always acquired as a proof of the correct proton energy by checking the maximum energy of the neutrons. Figure 7 shows all the spectra of the present work corrected by solid angle (black lines) compared to Lederer et al. (red lines).

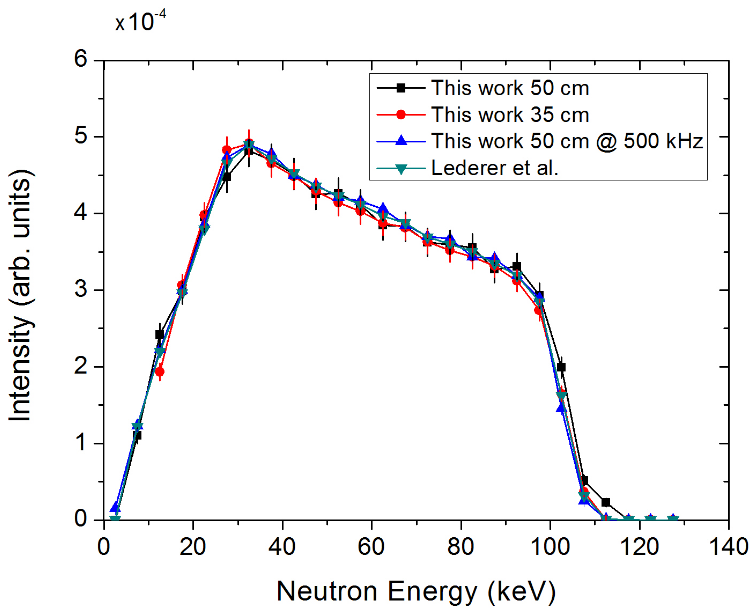

Figure 6: Experimental neutron spectra of this work at 0° at 50 cm flight path at 62.5 kHz (black line+squares), at 35 cm flight path at 62.5 kHz (red line+circles) and at 50 cm flight path at 500 kHz (blue line+triangles) compared to Lederer et al.(Lederer et al., 2012) (green line+triangles) in bins of 5 keV. Uncertainties given are statistical. In case of 50 cm flight path at 500 kHz the uncertainties are lower than the blue triangle.

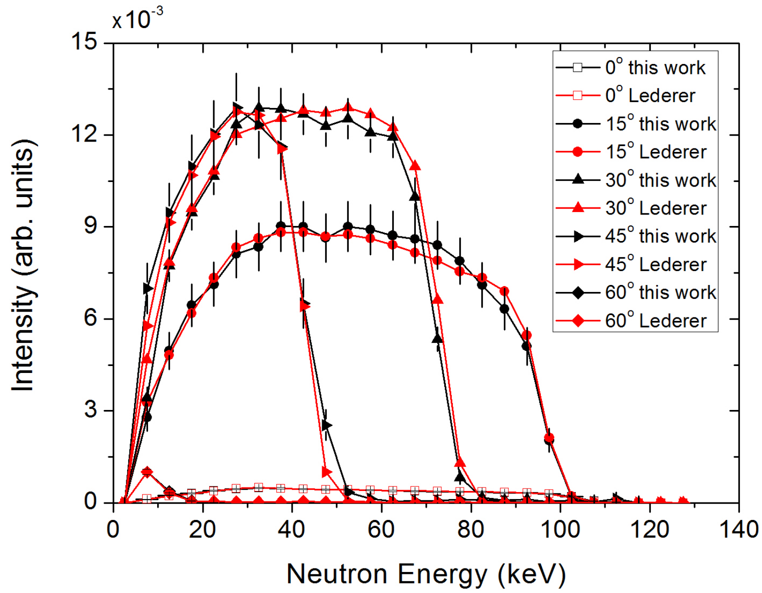

Figure 7: Black lines: present work, experimental neutron spectra from 0° to 60° in steps of 15°. Red lines: experimental neutron spectra of Lederer et al. (Lederer et al., 2012) in bins of 5 keV. Spectra are corrected by the corresping solid angle. Open points correspond to 0° which were discussed in Fig. 6. Uncertainties given are statistical.

As mentioned before, the correction at 0° is the most important. In spite of the lower statistics in our experiment, the agreement in the shape of the spectra and in the maximum energy is very good within statistical uncertainties. Also the relative intensity between our spectra is in a very good agreement with the relative intensity of the Lederer et al. spectra. The very small differences are justified due to the possible deviation of the proton energy in the experiment of Lederer et al., as it was noticed by the authors (Lederer et al., 2012). The comparison of our results with Lederer et al. guarantees the good performance of the TOF system and data acquisition for neutrons installed at CNA.

The integration over the entire neutron cone of the spectra corrected by the respective solid angle gives the angle-integrated spectrum at the neutron production point, thus, the R&K field. As it has been mentioned, the R&K

field has been extensively used since 1988 in nuclear astrophysics because it resembles in good approximation the neutron field during He shell flashes in AGB stars (Colonna et al., 2018). Indeed, stellar neutron-induced cross sections (or MACS) have been determined on 120 isotopes with the R&K field according to the KADoNiS compilation (Dillmann et al., 2014). The excellent stability of the R&K field and the agreement between the measurements of R&K, Lederer et al. and Feinberg et al. carried out in three facilities with slightly different setups pushes more experimental work for its possible definition as a standard neutron field. One of the reason behind is that experimental MACS can also be used for the validation of nuclear data libraries in the 10-120 keV range that is important in the description of fast neutron systems (e.g. Gen-IV nuclear reactors) (Praena et al., 2014).

It is straightforward that the good agreement shown in Figures 6 and 7 will provide also a good agreement in the angle-integrated spectrum. Nevertheless, the measurement of R&K (Ratynski et al., 1988) included two more angles than our measurement. In order to compare properly the angle-integrated spectra, we simulated the spectra of the missing angles following the procedure explained in section 3 (Praena et al., 2014) and we added them to our experimental ones. Figure 8 shows the angle-integrated spectrum obtained in the present work compared to R&K (Ratynski et al., 1988). The energy binning selected in each experiment was kept. Both spectra were normalized to the same area. It can be noticed that our result and the R&K field are in a good agreement within uncertainties (dashed lines). This is a further confirmation of the good performance of the whole TOF system.

Finally, Table 1 summarizes the main parameters of TOF line for neutrons at CNA. The energy resolution ($\Delta E/E$) is shown at relevant energies for 1 nsec pulse width and 50 cm flight path. The average intensities of the proton beam on the target were obtained at the selected repetition rates by measuring the integral charge on target. The uncertainty of the average intensity corresponds to the sensibility of the current integrator. The corresponding average proton current in continuous mode was 5 μA.

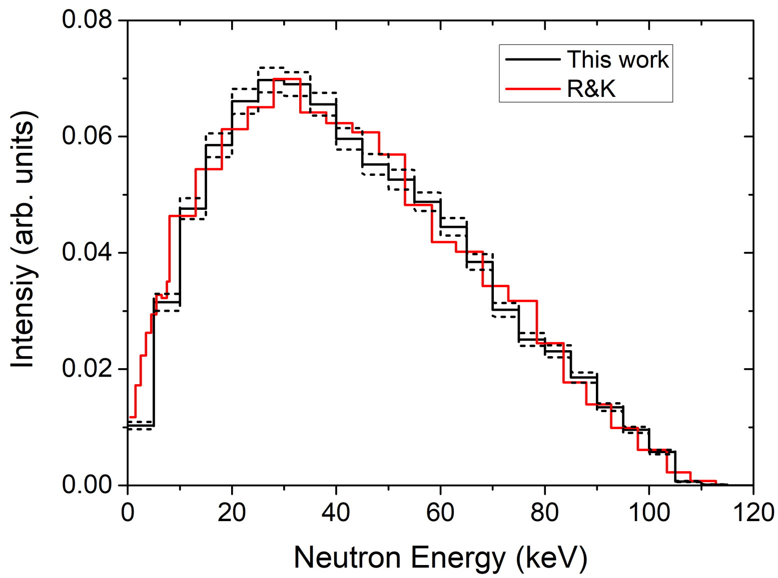

Figure 8: Final angle-integrated neutron spectrum. Black histogram corresponds to our work (experimental+simulation), red histogram corresponds to Ratynski and Käppeler (R&K) (Ratynski et al., 1988). Both spectra are normalized to the same area. Uncertainties given are statistical (dashed lines).

Table 1: Summary of the main parameters of the neutron TOF line at CNA. Energy resolution at selected energies were calculated for 50 cm flight path and 1 nsec pulse width. Average proton intensities on target were measured for 5 μA current in continuous mode. Uncertainties given correspond to the sensitivity of the integrator.

Energy (keV)	$\Delta E/E$	Repetition Rate (kHz)	Average Intensity (nA)
1	$1.8{\cdot}10^{-3}$	62.5	18±2
30	$9.7{\cdot}10^{-3}$	125	37±4
100	$1.8{\cdot}10^{-2}$	500	130±13
1000	$5.6{\cdot}10^{-2}$	2000	500±50

The aim of the the present work was to test the performance of the TOF system. For this reason, the spectra were measured at different flight paths and repetition rates. However, it is possible to provide information about the neutron flux available at CNA for future TOF experiments with the setup of the present experiment. Considering that the neutron yields of the ^{7}Li(p,n)^{7}Be reaction with protons from near-threshold to 2.5 MeV onto a thick lithium target were reported by Lee and Zhou (Lee et al., 1999), 6 neutrons/pulse can be produced with 1912 keV protons at 500 kHz when the current in continuous mode is 5 μA.

5. Conclusions

Since few years ago in Spain, the National Accelerator Laboratory (CNA) is developing a program in the field of experimental neutron physics. Several experiments have been carried out in continuous beam at the 3 MV Tandem Pelletron accelerator with application to nuclear astrophysics, dosimetry and studies on Single Event Effects on electronic devices. In the last years, the efforts have been focused in the design and setup of a new line dedicated to experiments involving neutrons by means of the time-of-flight technique. For this, a system consisting of a chopper and a buncher was installed at the low energy of the accelerator, upstream the tandem tank. The chopper provides pulsed beams up to 60 ns of duration with variable repetition rate from 62.5 kHz to 2 MHz. The buncher is able to compress in time the beam to one nanosecond pulse width (FWHM). Also, a new line has been installed downstream the accelerator tank and an acquisition system based on a CAEN Digitizer has been prepared. In order to demonstrate the performance of the whole system, we have measured the well-known neutron field generated by the ^{7}Li(p,n)^{7}Be reaction with protons at 1912 keV onto a thick target by means of the TOF technique. The results of the analysis are in agreement with Ratynski and Käppeler (R&K) (Ratynski et al., 1988) and Lederer et al. (Lederer et al., 2012) confirming the good performance of the whole TOF system at CNA.

The angle-integrated spectrum of R&K has been extensively used in nuclear astrophysics since 1988 and it is known as R&K field or *quasi*-stellar neutron spectrum at kT=25 keV. At present, the R&K field is on the road map to be defined as a neutron standard. The present measurement at CNA may contribute to such definition in the future.

6. Acknowledgements

The authors thank A.J. Romero and J.A. Labrador for the high quality of the proton beam and their help during the experiment. We acknowledge financial support for this work from the Spanish MINECO and FEDER funds under contract FIS2015-69941-C2-1-P, FPA2016-77689-C2-1-R, Asociación Española Contra el Cáncer (AECC) under contract PS16163811PORR, Junta de Andalucía under contract P11-FQM-8229, and the Fundación ACS.

References

CAEN, 2016. User Manual UM3148 DT5730/DT5725 8-Channel 14-bit 500/250 MS/s Digitizer. URL: https://www.caen.it/products/dt5730/

Colonna, N., Gunsing, F., Käppeler, F., 2018. Neutron physics with accelerators. Prog. Part. Nucl. Phys. 101, 177203.

Carlson, A.D., Pronyaev, V.G., Capote, R., et al., 2018. Evaluation of the Neutron Data Standards. Nuclear Data Sheets 140, 143-188.

Dillmann, I., Plag, R., Käppeler, F., et al., 2014. The new KADoNiS v1.0 and its influence on the weak s-process nucleosynthesis Proceedings of Science (NIC XIII) 57.

Feinberg, G., Friedman, M., Krása, A., et al., 2012. Quasi-stellar neutrons from the ^{7}Li(p,n)^{7}Be reaction with an energy-broadened proton beam. Phys. Rev. C85, 055810.

Friedman, M., Cohen, D., Paul, M. et al., 2013. Simulation of the neutron spectrum from the ^{7}Li(p,n) reaction with a liquid-lithium target at Soreq Applied Research Accelerator Facility. Nuc. Inst. and Met. in Phys. Res. A 698, 117-126.

García-López, F.J., Ager, F.J., Barbadillo, M., Madrigal, F.J., Ontalba, M.A., Respaldiza, M.A., Ynsa, M.D., 2000. CNA: the first accelerator-based IBA facility in Spain. Nucl. Inst. and Met. in Phys. Res. B 161-163: 1137-1142.

Gunsing, F., et al, The n_TOF Collaboration, 2016. Nuclear data activities at the n_TOF facility at CERN. Eur. Phys. J. Plus 131: 371.

Irazola, L., Praena, J., Fernández, B., Macías, M., Bedogni, R., et al., 2016. Using a Tandem Pelletron accelerator to produce a thermal neutron beam for detector testing purposes. Applied Rad. and Iso. 107, 330334.

Jiménez-Bonilla, P. and Praena, J., 2014. Measurement of the ^{197}Au(n,γ) stellar cross section at kT=30 keV by activation. Proceedings of Science (NIC XIII) 102.

Lederer, C., Käppeler, F., Mosconi, M., et al., 2012. Definition of a standard neutron field with the ^{7}Li(p,n)^{7}Be reaction. Phys. Rev. C 85, 055809.

Lee, C.L. and Zhou, X.-L., 1999. Thick target neutron yields for the ^{7}Li(p,n)^{7}Be reaction near threshold. Nuc. Inst. and Met. in Phys. Res. B 152, 1-11.

Liskien, H. and Paulsen, A., 1975. Neutron production cross sections and energies for the reactions ^{7}Li(p,n)^{7}Be and ^{7}Li(p,n)^{7}Be*. At. Data and Nuc. Data Tables 15, 57-84.

Macías, M., Fernández, B., Labrador, J.A., Romero, A. and Praena, J., 2019. Nanosecond pulsed proton beam: upgrade of the accelerator-based neutron facility HiSPANOS at CNA (Spain). Accepted for pubblication in Il Nuovo Cimento, https://arxiv.org/abs/1906.05716.

Macklin, R. L. and Gibbons, J. H., 1958. Study of the T(p,n)^{3}He and ^{7}Li(p,n)^{7}Be reactions. Physical Review 109, 1, 105-109

Malagón, D., Bota, S.A., Torrens, G., Gili, X., Praena, J., et al. 2017. Soft error rate comparison of 6T and 8T SRAM ICs using mono-energetic proton and neutron irradiation sources. Microelectronics Reliability 78, 38-45.

Mastinu, P.F., Martín-Hernández, G. and Praena, J., 2009. A method to obtain a Maxwell-Boltzmann neutron spectrum at kT=30 keV for nuclear astrophysics studies. Nuc. Inst. and Met. in Phys. Res. A 601, 333-338.

MCNPX code, Pelowitz, D.B., 2005. MCNPX USERS MANUAL Version 2.5.0 - LA-CP05-0369, Los Alamos National Laboratory LACP, 2005.

NEC, National Electrostatic Corp., http://www.pelletron.com.

Praena, J., Mastinu, P.F., Pignatari, M., et al., 2013. Measurement of the MACS of ^{181}Ta(n,γ) at kT=30 keV as a test of a method for Maxwellian neutron spectra generation. Nuc. Inst. and Met. in Phys. Res. A 727, 1-6.

Praena, J., Mastinu, P.F., Pignatari, M., et al., 2014. Measurement of the MACS of ^{159}Tb(n,γ) at kT=30 keV by activation. Nuclear Data Sheets 120, 205-207.

Praena, J., Irazola, L., Fernández, B., Macías, M., Bedogni, R., et al., 2015. Proposal of thermal neutron detector stability for peripheral dose estimation in clinac at a novel neutron facility. Rad. and Onco. 115 - S375.

Reifarth, R., Heil, M., Käppeler, F. and Plag, R., 2009. PINO - a tool for simulating neutron spectra resulting from the ^{7}Li(p,n)^{7}Be reaction. Nuc. Inst. and Met. in Phys. Res. A 608, 139-143.

Scionix Ltd., Regulierenring 5, 3981 LA Bunnik, The Netherlands. URL: https://scionix.nl/

Ratynski, W. and Käppeler, F., 1988. Neutron capture cross-section of ^{197}Au: A standard for stellar nucleosynthesis. Phys. Rev. C 37, 595-604.